Speckle contrast from the split-and-delay unit with seeded X-ray pulses of the MID instrument at European XFEL

Journal of Physics: Conference Series **3010** (2025) 012173 doi:10.1088/1742-6596/3010/1/012173

Speckle contrast from the split-and-delay unit with seeded X-ray pulses of the MID instrument at European XFEL

Claudia Goy[1*], Francesco Dallari[2] , Wojciech Roseker[1], Robert P.C. Bauer[1,3], Sharon Berkowicz[4], Bertram Friedrich[5], Alexander Gierke[1,5], Niels C. Giesselmann[1], Wonhyuk Jo[5], Wei Lu[5], Johannes Möller[5], Jan-Etienne Pudell[5], Angel Rodriguez-Fernandez[5], Roman Shayduk[5], Nele N. Striker[1], Joana Valerio[5], Mohamed Youssef[5], Alexey Zozulya[5], Paul Fuoss[6], Christian Gutt[7], Joachim Schulz[5], Gregory B. Stephenson[8], Anders Madsen[5], Gerhard Grübel[5], Fivos Perakis[4], and Felix Lehmkühler[1,9]

[1] Deutsches Elektronen-Synchrotron DESY, Hamburg, Germany
[2] Department of Physics and Astronomy, University of Padua, Padova, Italy.
[3] Freiberg Center for Water Research, TU Bergakademie Freiberg, Freiberg, Germany
[4] Department of Physics, Stockholm University, Stockholm, Sweden
[5] European X-ray Free Electron Laser Facility, Schenefeld, Germany
[6] Linac Coherent Light Source, SLAC National Accelerator Laboratory, Menlo Park, USA
[7] Department of Physics, Universität Siegen, Siegen, Germany
[8] Materials Science Division, Argonne National Laboratory, Argonne, USA
[9] The Hamburg Centre for Ultrafast Imaging, Hamburg, Germany

[*]E-mail: claudia.goy@desy.de

Abstract. We report on the coherence properties and characteristics of the split-and-delay unit at the Materials Imaging and Dynamics instrument of the European XFEL under seeded-beam conditions. Our investigation focuses on the speckle contrast extracted from the scattering patterns from static scatterers and pulse splitting characteristics. Seeded-beam operation enabled a high throughput of the split-and-delay unit. We highlight the invaluable potential of the split-and-delay unit for experimental investigations for enhancing our understanding of ultrafast phenomena in molecular liquids, such as water and aqueous solutions.

1. Introduction

The split-and-delay unit (SDL) at the Materials Imaging and Dynamics (MID) instrument of the European X-ray Free Electron Laser (EuXFEL) represents a promising tool for probing ultrafast dynamics at the molecular level. This device enables the splitting of a single FEL pulse into two fractions, with a controllable delay between them ranging from -10 ps up to 800 ps with a few fs precision [1] following the approach of Roseker et al. [2]. This timing range enables the ability to investigate dynamic processes that have been challenging to access experimentally, particularly in important molecular liquids like water and aqueous solutions [3]. These substances exhibit critical temperature- and concentration-dependent dynamics on the picosecond timescale, crucial for understanding ultrafast phenomena. One prime example is the self-intermediate

scattering function (SISF) of molecular water. Molecular dynamics simulations predict that water undergoes a two-step relaxation process at supercooled temperatures, with the second step occurring around 1 ps at room temperature and shifting to longer times with decreasing temperature [4]. The SDL unit's ability to finely tune the pulse delay within this time window allows for experimental validation of these predictions. Previous measurements using split-and-delay optics at SACLA and LCLS have demonstrated the feasibility of these types of experiments, such as on pure water, highlighting the SDL techniques potential for advancing studies of molecular liquids [5]–[9].

The development of X-ray FELs has advanced time-domain X-ray photon correlation spectroscopy (XPCS) experiments towards providing direct access to the SISF of molecular systems. FEL-based XPCS enables the study of both short- and long-time dynamical processes, with the time windows defined by either the pulse length or the machine's repetition rate. At the EuXFEL, processes occurring at timescales of 4.5 MHz or slower can be explored in "sequential mode," [10]–[13], while short-time dynamics, down to the femtosecond scale, can be probed using X-ray speckle visibility spectroscopy (XSVS) mode through taking advantage of the provided short pulse length [14], [15]. The SDL unit allows covering the timescales in between by a split-pulse XSVS mode [10]. In this mode, X-ray speckle patterns generated from pairs of pulses separated by variable delays, typically less than a nanosecond, contain information about the structural dynamics on the probed timescale.

Central to both approaches (XSVS and XPCS) is the measurement and analysis of low-count-rate 2D speckle patterns. For XSVS, the measured speckle contrast β_{meas} is quantified by the variance of intensity on the detector:

$$\beta_{\mathrm{meas}}(q) = \frac{\langle I(q)^2 \rangle - \langle I(q) \rangle^2}{\langle I(q) \rangle^2} - \frac{1}{\langle I(q) \rangle} \tag{1}$$

where $\langle \dots \rangle$ denotes the spatial average over pixels within the same q-bin and $q = \frac{4\pi}{\lambda} \sin\left(\frac{\theta}{2}\right)$ the modulus of the momentum transfer, with the photon wavelength λ and the scattering angle θ.

Such SDL capabilities have been already demonstrated at other facilities such as LCLS under Self-Amplified Spontaneous Emission (SASE) operation [16], [17] and at SACLA [18] in seeded 30 Hz mode. EuXFEL offers a significant advantage over those sources due to its high pulse energies and, crucially, the ability to produce up to 27,000 pulses per second. Therefore, successful SDL operation at EuXFEL has the potential to surpass any other source as it allows more comprehensive data collection, increasing the precision and depth of ultrafast dynamic studies.

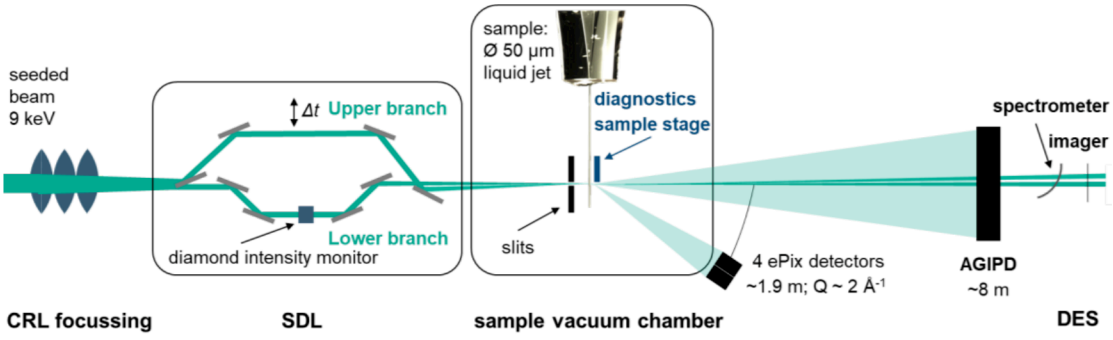

Figure 1. Beamline and measuring geometry of the experiment.

2. Method

Figure 1 shows the final optical scheme used during the experiment at MID. The measurement was done in the framework of experiment ID 3303 [19] that was focused on performing split-pulse XSVS on a liquid jet and here we discuss the characterization from a 100 µm thick Vycor glass sample in SAXS geometry. In this experiment, pulses with a photon energy of 9 keV were provided using hard X-ray self-seeding (HXRSS) [20]. At MID, the SDL [1] is located about 10 m upstream from the sample. It utilizes Si (220) crystal optics to split single FEL pulses in a horizontal geometry into an upper branch (UB) and a lower branch (LB), applying delays and overlapping both fractions at the sample position. A diamond intensity monitor recorded the beam intensity in the LB of the SDL. The pulse rate for utilizing the SDL was limited to 10 Hz during the experiment. The compound refractive lenses (CRL) were used to focus the beam to a beam size of about 20 ± 5 µm FWHM at the sample position. The Adaptive Gain Integrating Pixel Detector (AGIPD) was installed in SAXS geometry at about 8 m distance downstream the sample. The multipurpose diagnostic end-station (DES) [21] was running with an imager (YAG) and the spectrometer at the end of the instrument.

As described in the introduction, split-pulse XSVS monitors the variation of β_{meas} with the time delay Δt between the split pulses. Such split-pulse XSVS experiments encounter typically several challenges for the experimental design. One important aspect in the case of geometrical pulse splitting, as utilized in the SDL at MID, is the reduction of speckle contrast by the limited spatial overlap of both beam fractions at the sample as well as on the detector with implications described in detail by Sun et al. [22]. While by geometry, a full spatial overlap cannot be achieved, the focussing and SDL alignment have to be carefully tuned to obtain the maximum possible partial overlap of both beams at the sample and detector position.

Another challenge is the typically low photon flux at the sample position, which is partly constrained by the throughput of the SDL optics. This throughput can be enhanced by using self-seeding rather than the SASE operation mode of the FEL. With HXRSS, EuXFEL can produce pulses of 9 keV photon energy with a bandwidth of 0.8 eV FWHM and an average energy of 1.2 mJ compared to the standard SASE operation delivering FWHM bandwidths of about 20 eV at a pulse energy of 2.2 mJ [20]. Accordingly, seeded operation offers a significantly higher spectral density for SDL transmission. More importantly, a smaller photon energy bandwidth increases the

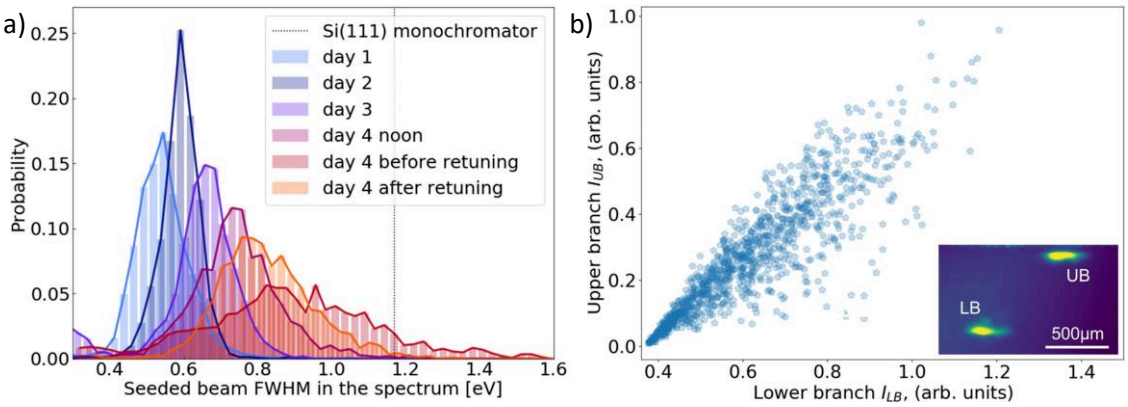

Figure 2. a) Histograms of the FWHM of the seeded beam for selected runs over the duration of the experiment and the estimated bandwidth of the Si (111) monochromator. b) Splitting ratio statistics of all pulses from a single run with a resulting $\langle r \rangle = 1.32$. The pulse intensities were diagnosed using the DES imager through integration of the intensity on an YAG screen, which is shown in the inset as an averaged image over the run with the locations of UB and LB indicated.

maximum speckle contrast at wide scattering angles. Other factors of the experiment and source properties affect the maximum speckle contrast like the degree of coherence of the FEL pulses, the sample thickness, the beam size on the sample, and the detector pixels size [15]. The seeding performance during the experiment is addressed by fig. 2a. It shows histograms of the FWHM of the first FEL pulses for selected runs on different days up to a maximum of 1500 pulses. The energy bandwidth was broadening over time, and retuning by the EuXFEL beam control was necessary, especially during the last day of the experiment. Thorough retuning affected also the photon energy with shifts around 0.1 eV. Such a slight change of the photon energy required careful realignment of the optics within the SDL. However, the comparison with the estimated bandwidth of a common Si (111) monochromator indicated by the vertical line in fig. 2a, shows that the seeded beam's bandwidth was consistently below that level throughout the experiment.

In split-pulse XSVS the two fractions of the FEL pulse that are forming the speckle pattern are not always of equal intensity. In this case, the measured speckle contrast is described by [23]

$$\beta_{meas}(q,\Delta t) = \beta_0 \frac{r^2 + 1 + 2r|f_0(q,\Delta t)|^2}{r^2 + 1 + 2r} \tag{2}$$

with the splitting ratio $r = I_{LB}/I_{UB}$ between the lower and upper branch, $f_0(q,\Delta t)$ the SISF of the system and β_0 the contrast value obtained from the static calibration sample measurement. For a static scatterer $f_0(q,\Delta t)$ equals one. Note that eq. (2) assumes full spatial overlap of the two split beams on the detector. Following [17] we can introduce a decorrelation factor σ into eq. (2) taking into account the partial spatial overlap. For a static scatterer in SAXS regime, we thus obtain:

$$\beta_{meas}(r,\sigma) = \beta_0 \frac{r^2 + 1 + 2r\sigma}{r^2 + 1 + 2r} \tag{3}$$

As r may vary for each FEL pulse, analysis on a shot-to-shot basis is required. Figure 2b) shows the analysis of the splitting ratio for each pulse of a single run, by integrating pulse intensities on the imager in the DES. For the selected run, the LB delivered statistically more intensity than UB which was likely due to an imperfect positioning of the beam splitter of the SDL. However, the total fluctuation of the splitting ratios within the run, which is more due to pointing fluctuations of the FEL source, shows a relatively small spread when comparing to SDL experiments at other sources [17].

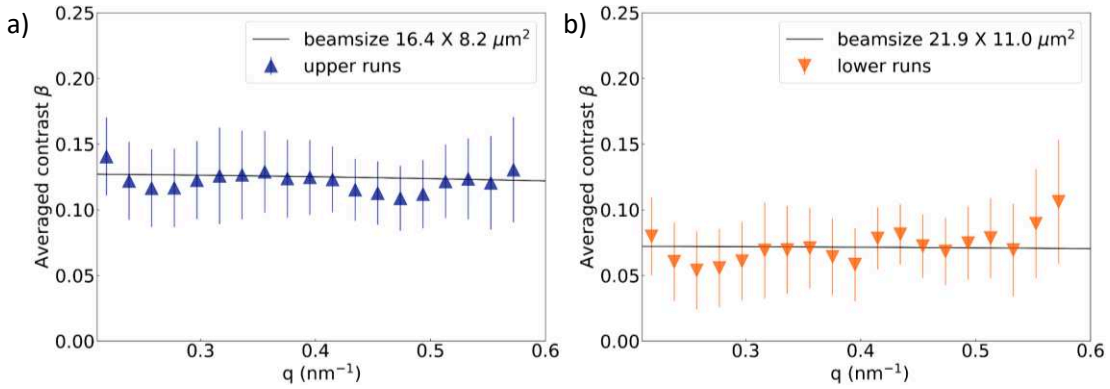

Figure 3. Speckle contrasts from the individual UB a) and LB b) of the SDL.

3. Results and Discussion

The contrast values were extracted from the photonized detector data as described in [24] for q-values between ~0.3 to 0.6 nm^{-1}, while for lower q the processed images in analog-to-digital units were used down to ~0.16 nm^{-1}. At low q the scattered intensity is relatively high so that "photonization" is not only unnecessary, but may introduce systematic errors for counts beyond 4 photons/pixel. Figure 3 shows the resulting speckle contrasts β of the single branches UB in a) and LB in b) at different q-values. For each configuration we took about 3300 pulses. We grouped the data and used $\langle I(q) \rangle$ to perform a weighted average, selecting only n regions of interests (ROI) with at least one two-photon event and adopting $1/\sqrt{n}$ to estimate the errorbars.

By considering the sample thickness of 100 µm, a sample to detector distance of 8 m, a pixel size of 200 µm and an estimated photon energy bandwidth $\Delta E/E = 6.6 \times 10^{-5}$ we can use the equation for estimation of the contrast reported in [22]. Assuming an aspect ratio of 2 between vertical and horizontal beam sizes we can fit eq. (3) to the $\beta(q)$ data and extract the beam size of both branches. We find about 16.4 µm (h) x 8.2 µm (v) for the UB and 21.9 µm x 11 µm for the LB, which is consistent with the estimated beam size determined with knife edge scans.

The analysis of about 4400 pulses with both branches is depicted in fig. 4. Figure 4a analyses the measured speckle contrast as a function of the splitting ratio r for a number of binned q-values. The black curves show a fit of the data with eq. (3) for each q-bin. The values were obtained by excluding ROIs on the detector with less than 10^{-3} ph/pixel. The average intensity of the ROI was used for a weighted average. The apparent minimum is located around the ideal splitting ratio around $r = 1$ as is expected for finite spatial overlap of both beams on the detector [17]. The corresponding fit results are shown for β_0 and σ in fig. 4b. The modulation of β_0 with q is consistent with the one observed for the single branch data. The β_0 being slightly larger than half of the single branch values indicates that partial overlap of the two branches on the sample and the detector was achieved. Also, the decorrelation factor fluctuating around a value between 0.1 and 0.15 is consistent with this assumption with an expectation value of 1 for full overlap and 0 for no overlap of the two beams. Equation (3) is valid when the two branches produce the same speckle contrast, but as can be seen from fig. 3 this condition is not exactly met. To account for this mismatch we considered the difference between the single branch contrasts in calculating the confidence bands of β_0.

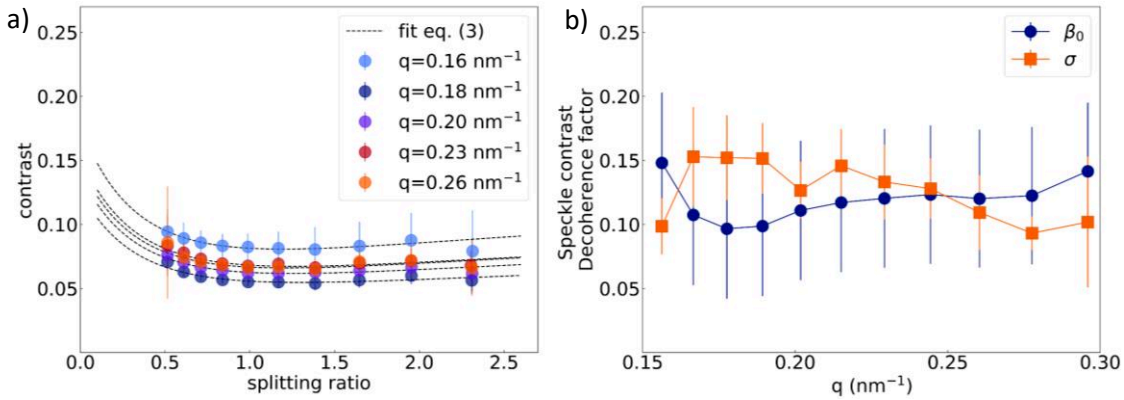

Figure 4. a) SDL contrast of both branches with Vycor sample and seeded beam as a function of splitting ratio for selected q-regions with the respective center q given in the legend. The dashed lines indicate a fit of eq. (3) to the data. b) q-dependence of the fit parameters contrast β_0 and overlap σ.

4. Conclusion

We presented the first static split-pulse speckle contrasts from the single and combined branches of the SDL at MID under seeded beam operation of EuXFEL. Achieving reasonable speckle contrast values and a partial spatial overlap of the two beams on both the sample and the AGIPD in SAXS geometry demonstrated the feasibility of split-pulse XSVS under seeded beam operation at MID. This experiment marks an important step toward achieving to the ultimate goal of studying picosecond dynamics of molecular liquids at EuXFEL. Next steps include reducing the beam size and the angular mismatch to increase the speckle contrast and advancing operation beyond 10 Hz and into WAXS geometry, where the relevant molecular liquid scattering occurs. This will allow the study of processes such as hydrogen bond dynamics in water and aqueous solutions which are believed to play a key role in water's unique properties, including its numerous anomalies. As such, the SDL unit at MID is a highly promising tool for exploring dynamics in molecular liquids, opening new avenues to study the fundamental behaviour of water and other complex liquids.

Acknowledgments

We acknowledge European XFEL in Schenefeld, Germany, for provision of X-ray free-electron laser beamtime at Scientific Instrument MID under proposal number P003303 [19] and would like to thank the staff for their assistance. This work was carried out in the framework of the 2022 EuXFEL Call on Molecular Water Science. We also acknowledge the scientific exchange and support of the Centre for Molecular Water Science (CMWS). This research was supported in part through the Maxwell computational resources operated at Deutsches Elektronen-Synchrotron DESY, Hamburg, Germany. This work is supported by the Cluster of Excellence 'Advanced Imaging of Matter' of the Deutsche Forschungsgemeinschaft (DFG) - EXC 2056 - project ID 390715994. PF was supported by U.S. DOE under Contract No. DE-AC02-76SF00515.

References

[1] W. Lu *et al.*, *Rev. Sci. Instrum.*, **89**, 6, 063121, (2018)
[2] W. Roseker *et al.*, *Opt. Lett.*, **34**, 12, 1768, (2009)
[3] F. Lehmkühler, W. Roseker, and G. Grübel, *Appl. Sci.*, **11**, 13, 6179, (2021)
[4] P. Gallo, D. Corradini, and M. Rovere, *J. Chem. Phys.*, **139**, 20, 204503, (2013)
[5] Y. Shinohara *et al.*, *Nat. Commun.*, **11**, 6213, (2020)
[6] Y. Sun *et al.*, *Phys. Rev. Lett.*, **127**, 5, 58001, (2021)
[7] E. Zarkadoula, Y. Shinohara, and T. Egami, *Phys. Rev. Res.*, **4**, 1, 13022, (2022)
[8] T. Fujita *et al.*, (2023) [Online]. Available: http://arxiv.org/abs/2312.08613
[9] P. Muhunthan *et al.*, *Rev. Sci. Instrum.*, **95**, 1, (2024)
[10] G. Grübel, G. B. Stephenson, C. Gutt, H. Sinn, and T. Tschentscher, *Nucl. Instruments Methods Phys. Res. Sect. B Beam Interact. with Mater. Atoms*, **262**, 2, 357, (2007)
[11] F. Lehmkühler *et al.*, *Proc. Natl. Acad. Sci.*, **117**, 39, 24110, (2020)
[12] M. Reiser *et al.*, *Nat. Commun.*, **13**, 5528, (2022)
[13] F. Dallari *et al.*, *Sci. Adv.*, **10**, eadm7876, (2024)
[14] C. Decaro *et al.*, *J. Synchrotron Radiat.*, **20**, 2, 332, (2013)
[15] F. Perakis *et al.*, *Nat. Commun.*, **9**, 1917, (2018)
[16] D. Zhu *et al.*, *Adv. X-ray Free. Lasers Instrum. IV*, **10237**, 650, 102370R, (2017)
[17] W. Roseker *et al.*, *Nat. Commun.*, **9**, 1704, (2018)
[18] T. Hirano *et al.*, *J. Synchrotron Radiat.*, **25**, 1, 20, (2018)
[19] DOI:10.22003/XFEL.EU-DATA-003303-00,
[20] S. Liu *et al.*, *Nat. Photonics*, **17**, 11, 984, (2023)
[21] U. Boesenberg *et al.*, *J. Synchrotron Radiat.*, **31**, 3, 596, (2024)
[22] Y. Sun *et al.*, *Phys. Rev. Res.*, **2**, 2, 023099, (2020)
[23] C. Gutt *et al.*, *Opt. Express*, **17**, 1, 55, (2009)
[24] F. Dallari *et al.*, *Appl. Sci.*, **11**, 17, 8037, (2021)